JACS
JOURNAL OF THE AMERICAN CHEMICAL SOCIETY
Article
pubs.acs.org/JACS

Long-Range Effects on the Capture and Release of a Chiral Guest by a Helical Molecular Capsule

Yann Ferrand,[†,¶] Nagula Chandramouli,[†,¶] Amol M. Kendhale,[†,¶] Christophe Aube,[§] Brice Kauffmann,[‡,#,∥] Axelle Grélard,[†,¶] Michel Laguerre,[†,¶] Didier Dubreuil,[§] and Ivan Huc*[,†,¶]

[†]Université Bordeaux, CBMN, UMR 5248, Institut Européen de Chimie Biologie, 2 rue Escarpit 33607 Pessac, France
[¶]CNRS, CBMN, UMR 5248, Institut Européen de Chimie Biologie, 2 rue Escarpit 33607 Pessac, France
[§]Université de Nantes, CNRS, Chimie et Interdisciplinarité: Synthèse, Analyse, Modélisation, UMR CNRS 6230, Faculté des Sciences et des Techniques, 2 rue de la Houssinière, BP 92208, 44322 Nantes Cedex 3, France
[‡]Université Bordeaux, Institut Européen de Chimie Biologie, UMS 3033/US 001, F-33600 Pessac, France
[#]CNRS, Institut Européen de Chimie Biologie, UMS 3033, F-33600 Pessac, France
[∥]INSERM, Institut Européen de Chimie Biologie, US 001, F-33600 Pessac, France

Supporting Information

ABSTRACT: Helically folded molecular capsules based on oligoamide sequences of aromatic amino acids which are capable of binding tartaric acid in organic solvents with high affinity and diastereoselectivity have been synthesized, and their structures and binding properties investigated by ^{1}H NMR, X-ray crystallography, circular dichroism, and molecular modeling. We found that elongating the helices at their extremities by adding monomers remote from the tartaric binding site results in a strong increase of the overall helix stability, but it does not influence the host−guest complex stability. The effect of this elongation on the binding and release rates of the guest molecules follows an unexpected non-monotonous trend. Three independent observations (direct monitoring of exchange over time, 2D-EXSY NMR, and molecular modeling) concur and show that guest exchange rates tend to first increase upon increasing helix length and then decrease when helix length is increased further. This investigation thus reveals the complex effects of adding monomers in a helically folded sequence on a binding event that occurs at a remote site and sheds light on possible binding and release mechanisms.

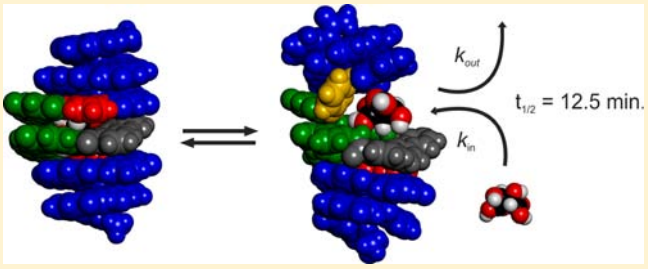

INTRODUCTION

Helically folded capsules based on aromatic oligoamides define an original class of molecular containers that can completely surround their guest and isolate it from the external medium.[1] Recent results by our group have shown that such receptors allow targeting of small chiral and polar guests with high affinity, selectivity, and diastereoselectivity.[2] The absence of any passage in the folded capsule wall implies that guest binding and release occur via a partial unfolding of the helix (Figure 1).

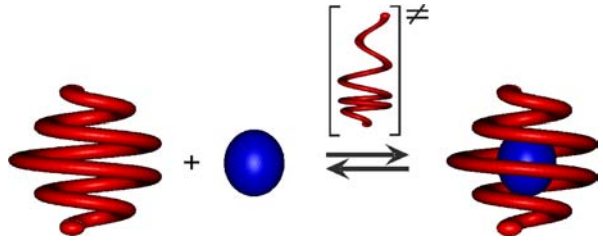

Figure 1. Encapsulation of a guest by partial unfolding of a helix possessing a reduced diameter at both ends.

This process is relatively slow due to the high stability of the helical conformations. For example, right-handed (*P*) and left-handed (*M*) helices of oligoamides of 8-amino-2-quinoline-carboxylic acid have been shown to interconvert, and thus to transit through partially unfolded states, with half-lives that range from minutes to hours, days, and even months when their length increases.[3] Such partially unfolded states would allow a guest to enter (or escape from) a cavity. In this respect, helical capsules differ from most helically folded receptors with an open cavity in which a guest may rapidly enter.[4] As an exception, it has been shown that guests with a dumbbell shape also require helix unfolding to bind to a helical receptor with an open cavity; a sliding mechanism of guest binding and release is proscribed, and slow kinetics result from the barrier to unfold the receptor.[5] Analogies can also be drawn between helical capsules and other types of molecular capsules such as hydrogen-bonded host complexes (for example "soft-balls"),[6−8] (hemi)carcerands,[9−11] cryptophanes,[12] and other self-assembled organometallic cages.[13−15] In these systems,

Received: May 4, 2012
Published: June 12, 2012

   dx.doi.org/10.1021/ja304322c | *J. Am. Chem. Soc.* 2012, 134, 11282−11288

guest exchange to and from the host is also governed by dynamic conformational or structural changes. Examples include "gating" and "slippage" mechanisms, or the complete dissociation of the receptor.[16]

Aromatic oligoamide helical capsules resemble nature's receptor architectures in that they consist of self-organized (folded) sequences of various monomers.[17] This design offers considerable modularity since monomers can easily be replaced by others and sequences can be elongated without having to entirely revise the synthetic plan. In aromatic oligoamides, each monomer locally sets helix curvature and the functional groups that converge toward the helix cavity, which in turn determine the cavity size and molecular recognition properties, respectively. The slow kinetics of guest binding and release mentioned above hint at the possibility to develop fully controlled systems in which guest release may be triggered on demand. Intrigued by this perspective, we set out to explore the extent to which modifications of the sequence may alter guest binding and release rates. Our initial hypothesis was that additional monomers introduced at the end of the sequence, at locations remote from the receptor site, would not change the thermodynamics of binding. Yet, they would contribute to the overall helix stability via cooperative effects[3] and thus slow down guest binding and release kinetics. In the following, we present some evidence for a more complex trend. As predicted, monomers at remote locations do not influence the thermodynamics of guest binding. However, their effect on the kinetics is subtle: adding a few monomers at the end of a capsule sequence indeed results in slower kinetics but elongating the sequence further gives rise to fast kinetics again. These results shed light on the factors that govern the dynamic behavior of helical aromatic amide oligomers in solution and how a gate may open in a capsule wall for a guest to enter or leave the cavity. Thus, a very long helix may have an overall very stable structure and yet be subject to stronger conformation dynamics than a small helix, resulting in more frequent guest capture and release.

RESULTS AND DISCUSSION

Design and Synthesis. The first purpose of this study was to investigate the effect of elongating a helical-capsule sequence on its guest binding properties. Sequence **1** (Chart 1) has been

Chart 1. Formulas of Capsules 1, 2, 3, and 4 Together with the Abbreviations Used for Their Subunits

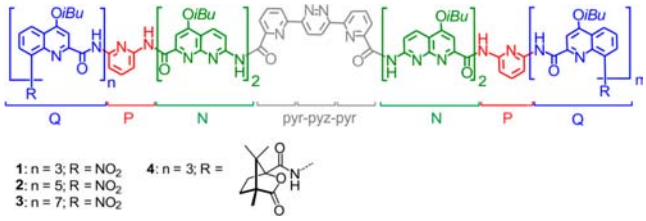

shown to be an efficient design of a helically folded capsule based on aromatic amino acids coding for a large helix cavity in the center of the sequence and a narrow helix diameter at the ends. It can bind tartaric acid[18] with high affinity and high diastereoselectivity (de > 99%) in organic solvents. As in other aromatic oligoamide foldamers, folding is driven by well-established local conformational preferences which set the preferred relative orientation of each amide group and adjacent aromatic units.[19] The binding site of the receptor is composed of three types of monomers, namely pyridine (**P**), naphthyridine (**N**), and the long pyridine−pyridazine−pyridine segment (**pyr-pyz-pyr**), all contributing to bring about specific structural and functional features. The quinoline (**Q**) trimers at each extremity of the strand are known to code for a strong curvature forming two caps closing the helix cavity.[20] Based on previous results,[3] we anticipated that the elongation of these quinoline segments would cause a dramatic increase of the overall stability of the helix. Hence, we designed two new sequences which include either a quinoline pentamer (**2**) or a quinoline heptamer (**3**) at each end of the sequence. As described earlier, a hexameric hemicapsule O_2N-$\mathbf{Q_3PN_2}$-Boc was convergently synthesized via the coupling of a O_2N-$\mathbf{Q_3}$-Cl acid chloride with the amino group of H_2N-$\mathbf{PN_2}$-Boc (see the Supporting Information (SI)). Two successive cycles of nitro group reduction, followed by coupling with a O_2N-$\mathbf{Q_2}$-Cl acid chloride, provided octamer O_2N-$\mathbf{Q_5PN_2}$-Boc and decamer O_2N-$\mathbf{Q_7PN_2}$-Boc in 94% and 95% yield, respectively. After quantitative Boc cleavage in the presence of trifluoroacetic acid (TFA), the three oligomers (O_2N-$\mathbf{Q_nPN_2}$-NH_2, with n = 3, 5, 7) were coupled to the 6,6′-diacid **pyr-pyz-pyr** segment[21] using benzotriazol-1-yl-oxytripyrrolidinophosphonium hexafluorophosphate (PyBOP) as coupling agent to give capsules **1** (91%), **2** (90%), and **3** (65%), as racemic mixtures of *P* and *M* enantiomers. Similarly, (1*S*)-(−)-camphanyl chloride was coupled to the hemicapsule H_2N-$\mathbf{Q_3PN_2}$-Boc to give camphanyl-$\mathbf{Q_3PN_2}$-Boc which, after Boc deprotection, was reacted with the diacid of **pyr-pyz-pyr** to give the chiral capsule **4** in good yield (73%). As shown previously, single camphanyl terminal groups result in quantitative helix handedness induction as far as NMR can detect.[22] Compound **4**, which possesses two camphanyl groups, was thus expected to fold exclusively as a *P*-helix.

Structural and Thermodynamic Study of Tartaric Acid Encapsulation. Single crystals of capsules **1**−**3** (free of any guest) were obtained from the slow evaporation of chloroform from a mixture of chloroform/DMSO (9/1), and their structures in the solid state were resolved in centrosymmetric lattices containing both *P* and *M* conformers (Figure 2A−C). The structures confirm the predicted canonical folding of the 17-unit-long (**2**) and 21-unit-long (**3**) capsules into well-defined helices as well as the conservation of the cavity shape at the center of the sequence (see SI): elongating the terminal quinoline segments does not much influence the conformation imparted by the central $\mathbf{PN_2}$-pyr-pyz-pyr-$\mathbf{N_2P}$ sequence. For example, the distances between the N1 nitrogen atoms of the two most central naphthyridine rings, which span the whole capsule cavity, are 8.72, 8.19, and 8.21 Å for **1**, **2**, and **3**, respectively.

To compare with the properties of **1**,[2] the ability of capsules **2** and **3** to bind D/L-tartaric acid was assessed in $CDCl_3$ using 1% DMSO-d_6 to dissolve the guest in the stock solution. For all capsules, guest binding and release was found to be slow on the NMR time scale at 298 K. In this solvent, the binding constants for receptors **1**−**3** were too high to be measured accurately through the integral ratios of the free and bound receptor signals. Quantitative binding of the guest to the host is observed after each addition until saturation is reached. Thus, the association constant (K_a) can be estimated to be higher than 10^6 L·mol^{-1} under these conditions. As observed for **1**⊃D/L-tartaric acid, a single set of well-resolved NMR signals was observed for the encapsulation of D/L-tartaric acid in **2** and **3** at equilibrium, indicating a completely diastereoselective inter-

dx.doi.org/10.1021/ja304322c | J. Am. Chem. Soc. 2012, 134, 11282−11288

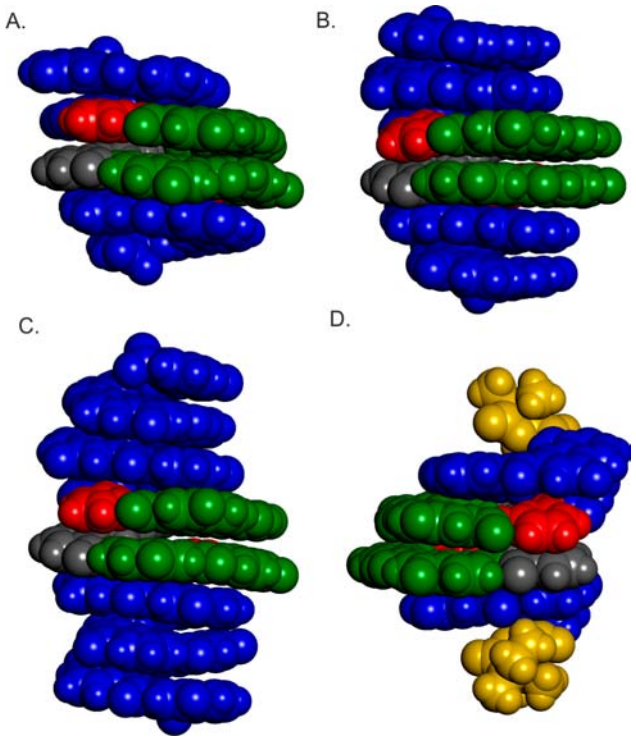

Figure 2. CPK representations of the solid-state structures of (A) the *M*-helix of **1** (Q_3PN_2-pyr-pyz-pyr-N_2PQ_3), (B) the *M*-helix of **2** (Q_5PN_2-pyr-pyz-pyr-N_2PQ_5), (C) the *M*-helix of **3** (Q_7PN_2-pyr-pyz-pyr-N_2PQ_7), and (D) the *P*-helix of **4** (camphanyl-Q_3PN_2-pyr-pyz-pyr-N_2PQ_3-camphanyl) with *S*-(−)-camphanyl moieties highlighted in gold at each end of the structure. Units are color-coded as in Chart 1. Isobutoxy groups and solvent molecules are not shown. The first three structures crystallized in centrosymmetric space groups and contained a racemic mixture of *P*- and *M*-helices, whereas the fourth crystallized in a chiral space group and contained only *P*-helices.

action (Figure 3). Each enantiomer of the guest was encapsulated by a helix having a unique handedness (see below). Remarkably, the ^{1}H NMR spectra of the host−guest complexes feature an overall upfield shift of all signals, including those of the bound guest, upon increasing the length of each quinoline segment at the extremities of the capsule. For instance, the sharp signal which resonates at 14.1 ppm in the spectrum of **1**⊃D/L-tartaric acid was previously assigned to the hydrogen-bonded tartaric acid protons. This signal is found at 13.85 ppm in the spectrum of **2**⊃D/L-tartaric acid and at 13.65 ppm in that of **3**⊃D/L-tartaric acid. This phenomenon has also been observed in Q_n sequences.[3] Presumably, it results from an addition of ring current effects as the stack of quinoline rings becomes thicker. The effect is long-range since signals of the guest are upfield shifted even though the guest lies about 1 nm away from the most peripheral quinoline rings in **3**.

Titrations of **1**−**3** with D/L-tartaric acid were carried out in a more polar solvent mixture ($CDCl_3$:d_6-DMSO 80:20 vol/vol) to decrease the binding constants down to values at which they can be accurately measured (Figure 4). In this medium, K_a values were found to be around 950 L·mol^{-1} for **1**−**3**, showing that the additional quinoline units in **2** and **3** have essentially no effect on the thermodynamics of tartaric acid binding, despite the long-range ring current effects mentioned above.

Diastereoselectivity of tartaric acid encapsulation by these helical receptors was assessed both in the solid state and in solution. Previously, single crystals of **1**⊃D/L-tartaric acid

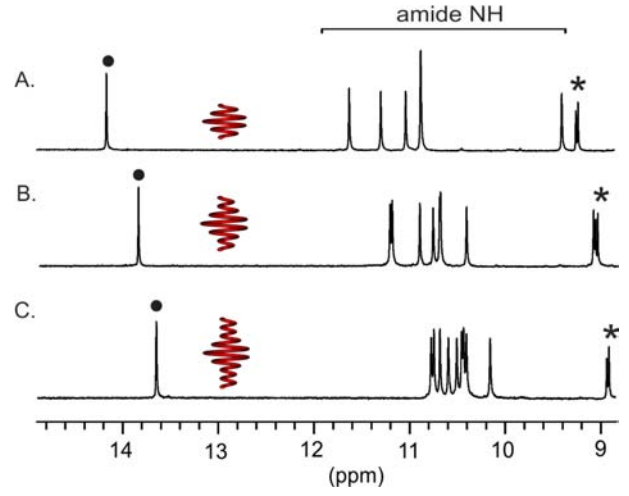

Figure 3. Part of the 700 MHz ^{1}H NMR spectra of (A) 13mer **1**, (B) 17mer **2**, and (C) 21mer **3** at 2 mM in $CDCl_3$:d_6-DMSO 99:1 vol/vol at 298 K in the presence of 1 equiv of D/L-tartaric acid. The sharp signal around 14 ppm is that of the hydrogen-bonded acid protons of the guest and is marked with a black circle. The star indicates an aromatic proton resonance. The resonances of the host and of the guest protons shift to higher fields when the sequence is elongated.

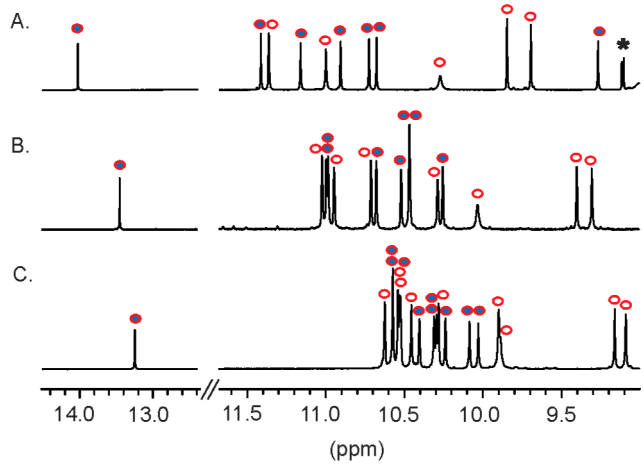

Figure 4. Part of the 700 MHz ^{1}H NMR spectra of (A) 13mer **1**, (B) 17mer **2**, and (C) 21mer **3** at 1.8 mM in $CDCl_3$:d_6-DMSO 80:20 vol/vol) at 318 K in the presence of 1 equiv of D/L-tartaric acid. Signals of the empty host and of the host−guest complex are marked with empty red and blue-in-red circles, respectively.

showed that D-tartaric acid was encapsulated in the *P*-enantiomer of **1** and, conversely, L-tartaric acid in the *M*-enantiomer.[2] This result was found to be consistent with the diastereoselectivity observed in solution by ^{1}H NMR. In order to get an accurate estimate of chiral discrimination, we introduced chiral capsule **4**. Single crystals of **4** were grown by slow diffusion of hexane into a chloroform solution, and its structure was elucidated in the $P2_12_12_1$ chiral space group (Figure 2D). In the solid state, **4** is exclusively right-handed, as expected from the handedness induction by (1*S*)-(−)-camphanyl groups.[22] This is confirmed in solution by the presence of a single set of ^{1}H NMR signals and by intense circular dichroism (CD) bands (Figure 5D,E). We could not obtain single crystals of **4** encapsulating either D or L-tartaric acid that were suitable for crystallographic analysis. Nevertheless, these host−guest interactions could be assessed in solution. A ^{1}H

dx.doi.org/10.1021/ja304322c | J. Am. Chem. Soc. 2012, 134, 11282−11288

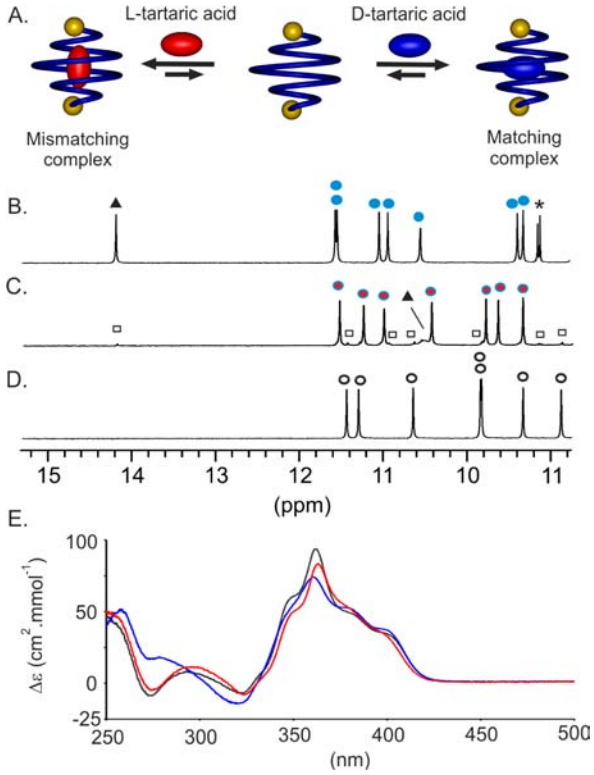

Figure 5. (A) Schematic representation of the encapsulation of D- or L-tartaric acid within a chiral helical capsule **4** whose handedness (*P*-enantiomer) is determined by two camphanyl moieties at each extremity (golden balls). (B–D) Part of the 300 MHz ^{1}H NMR spectra of **4** (2 mM in $CDCl_3$:d_6-DMSO 99:1 vol/vol) at 298 K in the presence of 1.1 equiv of *D*-tartaric acid (B), in the presence of 1.1 equiv of L-tartaric acid (C), and in the absence of guest (D). Signals of the empty host are marked with empty black circles. Signals of *P*-helix⊃D-tartaric acid are marked with blue circles and those of *P*-helix⊃L-tartaric acid are marked with red-in-blue circles. Empty squares denote a small amount of a matching complex. Triangles show signals of the hydrogen-bonded acid protons of the guest. (E) CD spectra of **4** (black), **4**⊃D-tartaric acid (blue), and **4**⊃L-tartaric acid (red) in $CHCl_3$/d_6-DMSO 99:1 vol/vol at 298 K.

NMR (700 MHz) titration of **4** with D-tartaric acid, which is expected to bind preferentially to the *P*-helix, was carried out in $CDCl_3$ with 1% DMSO-d_6 (Figure 5B). A single encapsulation complex formed quantitatively whose spectrum was very similar to those observed for capsules **1**–**3**, and whose CD trace matched that of empty **4** (Figure 5E). Accordingly, this new complex was assigned to *P*-**4**⊃D-tartaric acid. In contrast, titration with L-tartaric acid also gave rise to a new set of NMR signals corresponding to a host–guest complex but with a different pattern from the previous ones. The most notable difference was the broadening and upfield shift of the sharp signal at 14.1 ppm (characteristic of the hydrogen-bonded acid of the guest in *P*-**4**⊃D-tartaric acid) to a broad signal at 10.5 ppm, suggesting a weaker hydrogen bonding between the host and L-tartaric acid. The CD spectrum of this complex also matches that of **4** (Figure 5E) allowing assignment of this complex to *P*-**4**⊃L-tartaric acid. This result contrasts with titrations of racemic helices **1**–**3** for which *P*-helix⊃L-tartaric acid is absent (or transient, see below) since L-tartaric acid quantitatively induces *M* handedness.[2] Apparently, the camphanyl groups prevail over tartaric acid in controlling the *P* handedness of **4**. Interestingly, an additional minor set of signals is observed during the titration of **4** with L-tartaric acid (white squares in Figure 5C) which features a sharp singlet at 14.1 ppm. This species likely corresponds to a small amount of *M*-**4**⊃L-tartaric acid in which the handedness of the helix has been inverted by tartaric acid despite the camphanyl groups, resulting in more favorable host–guest interactions.

In order to determine the respective stability of the two diastereoisomeric complexes, *P*-**4**⊃D-tartaric acid and *P*-**4**⊃L-tartaric acid, a more competitive solvent was used again (10% DMSO-d_6 in $CDCl_3$) to decrease the binding constants to a level at which ^{1}H NMR titrations are accurate. In this mixture, K_a values for D and L-tartaric acid were found to be 9000 and 800 L·mol^{-1}, respectively. In the following, we call *P*-helix⊃D-tartaric acid and its enantiomer *M*-helix⊃L-tartaric acid matching complexes, and the diastereomeric pair *P*-helix⊃L-tartaric acid and *M*-helix⊃D-tartaric mismatching complexes (Figure 5A). The matching complex of **4** is 1 order of magnitude more stable than its mismatching complex. This ratio is smaller than observed with **1**–**3**, suggesting that camphanyl groups have some influence on binding, though this is not obvious in the crystal structure of **4**. Of importance for the experiments described below, we note that the stability of the mismatching complexes may be substantial, even if it remains smaller than that of the matching complexes.

The conformational stability of the helices **1**–**3** was studied through measurements of their handedness inversion rate (k_{inv}).[3] Upon titrating **1**–**3**, which exist at equilibrium as a racemic mixture of *P*- and *M*-helices, with L-tartaric acid, we observed in each case the appearance of two new sets of peaks (Figure 6C) resembling the signals observed in solutions of **4** encapsulating D- or L-tartaric acid, respectively. In particular, one set of signals possesses a sharp singlet at low field and the other does not. Accordingly, the two sets of peaks were assigned to the matching (*M*-helix⊃L-tartaric acid) and mismatching (*P*-helix⊃L-tartaric acid) complexes (Figure 6A). Upon standing, signals of the mismatching complexes progressively decreased in intensity to finally disappear (Figure 6C–F) and intense CD signals emerge.[2] This phenomenon corresponds to the slow conversion of *P*-helices into *M*-helices driven by the higher stability of the matching complex. Helix handedness inversion proceeds through rotations about aryl-amide bonds, and the disruption of local conformation preferences and of interactions associated with aromatic stacking.[3] It thus entails partially unfolded intermediates, and its rate reflects the intrinsic conformational stability of a helix. Full handedness inversion proceeded within 3 h in the case of oligomer **2** (Figure 6, half-life ~23 min), whereas in the case of oligomer **1**, which is four quinoline units shorter, the inversion proceeded faster (90 min, half-life ~19 min). The amplitude of this effect is spectacular for the longest capsule **3**, with a half-life of 71 h, for which 2 weeks were needed to invert its handedness (see SI). These results therefore validate our initial hypothesis that elongating the sequences results in more stable helices.

Direct Observation of Guest Exchange over Time. Unlike in the experiments described above, when the *P*/*M* racemic mixture of helices of **1**–**3** is titrated with D/L-racemic tartaric acid, a racemic pair of matching complexes is expected to form quantitatively without requiring any helix handedness inversion. Nevertheless, during these titrations as well, another species assigned to mismatching complexes was observed and decayed rapidly (Figure 7). The transient appearance of mismatching complexes is unexpected and highly significant. It suggests that a given tartaric acid molecule does not

dx.doi.org/10.1021/ja304322c | J. Am. Chem. Soc. 2012, 134, 11282–11288

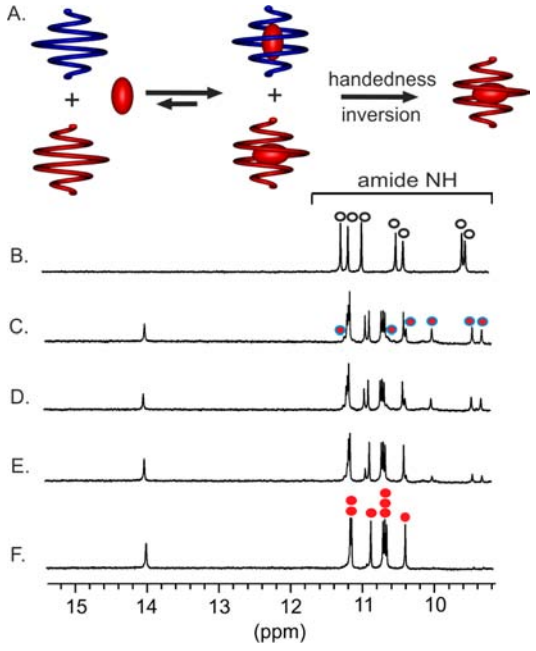

Figure 6. (A) Schematic representation of the encapsulation of a chiral guest (L-tartaric acid denoted in red) within a racemic helical capsule (*P* and *M* enantiomers are denoted in blue and red, respectively). (B–F) Part of the 300 MHz ^{1}H NMR spectra of **2** (2 mM in $CDCl_3/d_6$-DMSO 99:1 vol/vol) at 298 K before the addition of guest (B) and 4 min (C), 12 min (D), 58 min (E), and 184 min (F) after the addition of 1.1 equiv of L-tartaric acid. Signals of matching and mismatching diastereoisomeric complexes (*M*-helix⊃L-tartaric acid and *P*-helix⊃L-tartaric acid, respectively) are marked with red circles and red-in-blue circles, respectively. Empty black circles correspond to the empty capsule.

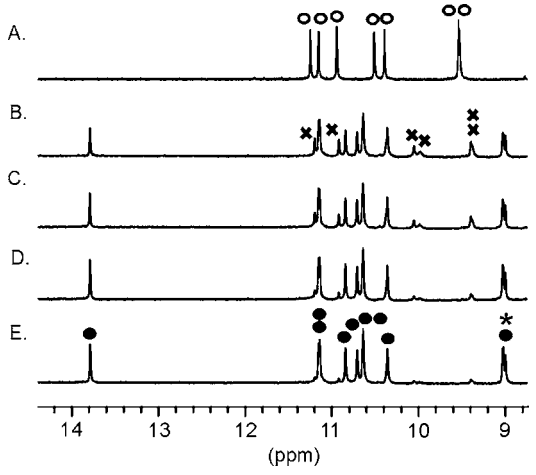

Figure 7. Excerpts of ^{1}H NMR spectra showing the discrimination as a function of time of the *P*- and *M*-helices of **2** by the two enantiomers of tartaric acid. Spectra were recorded at 273 K immediately after adding 1.1 equiv of D/L-tartaric acid to a solution of capsule **2** (2 mM, $CDCl_3/d_6$-DMSO 97.8:2.2 vol/vol). The selected window presents the amide resonances before the addition of guest (A) and 110 s (B), 300 s (C), 790 s (D), and 1000 s (E) after adding the guest. Amide signals of the empty capsule are marked with empty circles. Signals of matching complexes are marked with black circles whereas those of mismatching complexes are marked with crosses. An aromatic resonance is marked with a star.

discriminate the *P* or *M* handedness of a helix from the outside and may enter either one at comparable rates to form matching or mismatching complexes. Most likely, the two types of complexes differ by their guest release rates: because of their higher stability, the matching complexes dissociate at a slower rate than the mismatching complexes. In the titration shown in Figure 7, the D- and L-tartaric acid molecules initially distribute themselves randomly in the *P*- and *M*-helices. Equilibrium is reached as mismatching complexes dissociate and more matching complexes form (Figure 8).

The monitoring of this process as a function of time thus gives an estimate of the rates of guest exchange between capsules; more specifically, it reflects the rate of mismatching complex dissociation. This experiment was carried out with **1**–**3**, and we found that 5 min after the addition of D/L-tartaric acid, the percentage of remaining mismatching complex in solution is only 7% for **1**, 28% for **2**, and 12% for **3**. In the case of **1**, equilibrium is reached in about 15 min, after which time the signals of the mismatching complexes have disappeared (as far as NMR can detect). In the case of **2** (Figure 7), the process is slower, consistent with our initial hypothesis that elongating the sequences at positions remote from the binding site should stabilize the helix conformation and thus slow down guest exchange. However, in the case of the longest sequence **3**, this process becomes rapid again. This nonmonotonous trend clearly indicates that more than one factor is at play in determining guest binding and release rates. Helix stability alone as defined above (rate of helix handedness inversion) does not allow to make a prediction. Intrigued by these results, we set to explore guest exchange in more details and carried out the ^{1}H NMR and molecular modeling experiments described below.

Kinetics of the Encapsulation Process. The rates of encapsulation and dissociation were determined using EXSY NMR spectroscopy[23] for **1**–**3**. These experiments were carried out in presence of a large amount of DMSO (20%) so as to decrease binding and obtain an even ratio of full and empty capsules. In all cases, amide signals of the receptor encapsulating tartaric acid gave strong exchange cross-peaks with the corresponding amide of the empty capsule at 318 K. The magnetization constants for the encapsulation (k_{in}*) and release (k_{out}*) of tartaric acid for receptors **1**–**3** were obtained through the integration of cross and diagonal peaks (Figure 9). The encapsulation (k_{in}) and release (k_{out}) rates were then calculated as $k_{in} = k_{in}^*/[\text{capsule}]$ and $k_{out} = k_{out}^*$. The results summarized in Table 1 show significant differences between the different capsules and confirm the above observations: the rates of guest exchange, as a function of the length of the sequence, do not follow a monotonous trend. The rates of dissociation (k_{out}) of capsule **1** (0.110 s^{-1}) is twice as large as that of capsule **2** (0.055 s^{-1}), whereas the largest receptor **3** presents an intermediate kinetic stability (0.08 s^{-1}). Thus, guests escape faster from the longer sequence despite its larger overall conformational stability. The rates of complex formation (k_{in}) follow the same trend, and the binding constants (k_{in}/k_{out}) are found to be equal within experimental error for all foldamers. Thus, additional quinoline monomers are indeed found to have a significant remote effect on the guest binding and release rates, but this effect operates in a nontrivial manner: although longer sequences are overall more stable, this may not prevent the opening of windows near the binding site through which guests may enter or exit.

Molecular Dynamics. We gathered insights into the mechanistic details of the encapsulation process using molecular dynamics. Starting from a host–guest complex, as

dx.doi.org/10.1021/ja304322c | J. Am. Chem. Soc. 2012, 134, 11282–11288

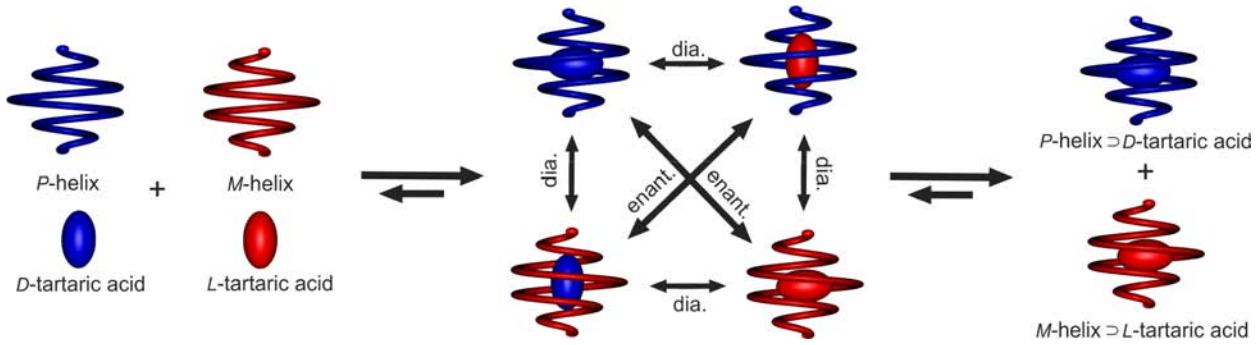

Figure 8. Schematic representation of the encapsulation of a racemic mixture of a guest molecule (D- and L-tartaric acid are in blue and red, respectively) within a racemic helical capsule (*P* and *M* handedness are denoted in blue and red, respectively). Encapsulation of the guest proceeds to give both the matching (blue-in-blue or red-in-red) and the mismatching (blue-in-red or red-in-blue) complexes. After equilibration only the matching complexes are observed which confirms a full diastereoselectivity.

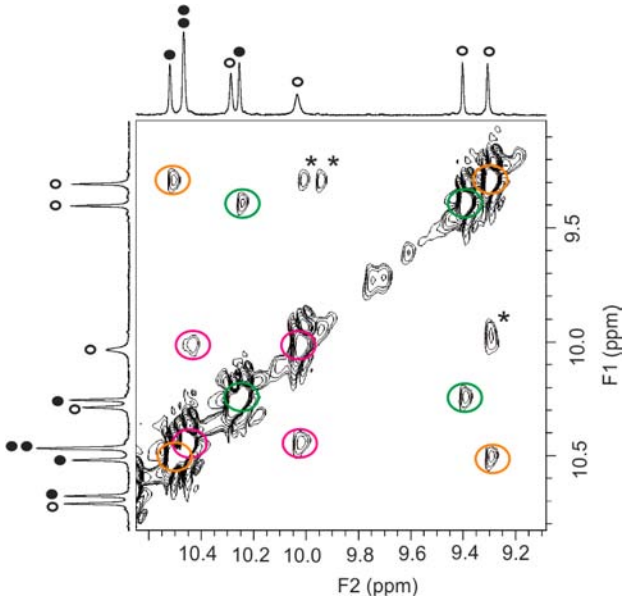

Figure 9. Downfield aromatic amide region of 2D-EXSY 700 MHz NMR spectrum of **2**⊃D/L-tartaric acid ([**2**] = 1.8 mM, [tartaric acid] = 1.8 mM in $CDCl_3/d_6$-DMSO 80/20 vol/vol, 318 K, τ_m = 300 ms). Signals of the empty host are marked with empty circles, whereas signals of **2**⊃tartaric acid are marked with black circles. Stars indicates the presence of a minor (<1%) diastereoisomeric complex.

observed in the X-ray structure of *P*-**1**⊃D-tartaric acid, 5 ns runs of molecular dynamics using a GB/SA continuum solvation model (see SI) were performed with increasing *in silico* temperatures until the guest was ejected during the course of the simulation. Quite remarkably, the trend was the same as experimentally observed. While tartaric acid was expelled from the binding site of **3** within 5 ns at temperatures of 900 K, or higher, it took higher temperatures (>1200 K) to trigger guest release in **2**. On the contrary, guest release was the fastest in the shortest sequences **1**. A careful examination of the conformations that lead to tartaric acid release recurrently shows that one terminal helical quinoline segment tilts away as a rigid block and opens a window in the capsule wall at the binding site, the neighbor pyridine unit playing the role of a hinge (Figure 10). This allows us to hypothesize on why guest binding and release could be faster in the longest and overall more stable helices: elongating the quinoline segments does lead to a local increase of the helix stability but does not prevent these segments from tilting away around the hinge. On the contrary, a larger compact terminal segment may be more exposed to local fluctuations associated with thermal energy, resulting in more frequent opening of the capsule cavity.

Table 1. Rate Constants for the Encapsulation (k_{in}, s^{-1} M^{-1}) and Release (k_{out}, s^{-1}) and Half-Life ($t_{1/2}$, s) of D/L-Tartaric Acid for Receptors 1−3 at 318 K ($CDCl_3/d_6$-DMSO 80/20)[a]

capsule	k_{in}[b]	k_{out}[b]	*Ka*	$\Delta G^{\ddagger}_{in}$[c]	$\Delta G^{\ddagger}_{out}$[d]	ΔG^{0}[e]	$t_{1/2}$[f]
1	105	0.110	954	15.72	20.05	4.34	3.1
2	50	0.055	909	16.19	20.49	4.30	12.5
3	73	0.080	913	15.95	20.25	4.31	8.7

[a]Free activation enthalpy of dissociation $\Delta G^{\ddagger}_{out}$ (kcal mol^{-1}) and association $\Delta G^{\ddagger}_{in}$ (kcal mol^{-1}) and free activation energy ΔG^0 (kcal mol^{-1}) were determined using the Eyring equation. [b]Determined by EXSY 2D NMR. [c]$\Delta G^{\ddagger}_{in} = -RT \ln(hk_{in}/k_BT)$. [d]$\Delta G^{\ddagger}_{out} = -RT \ln(hk_{out}/k_BT)$. [e]$\Delta G^0 = -RT \ln K$. [f]$t_{1/2} = \ln 2/k_{out}$.

CONCLUSION

In summary, the parallel investigation of three helical capsule sequences having identical binding sites but rigid segments of

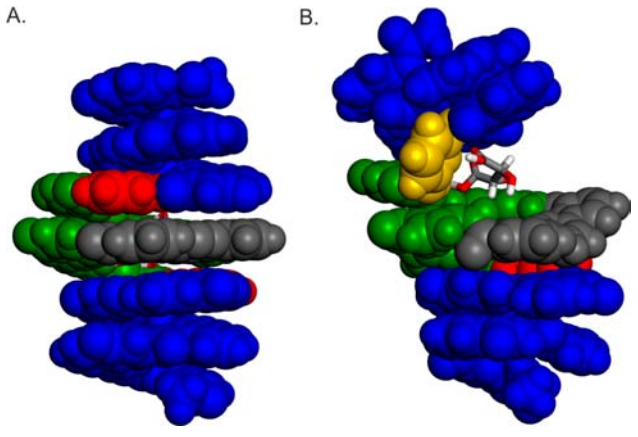

Figure 10. (A) Snapshot picture of capsule *P*-**2**⊃D-tartaric acid extracted from molecular dynamics simulation (GB/SA continuum solvation model) before heating. (B) Snapshot picture from the molecular dynamics of capsule **2**⊃tartaric at 1200 K after 2.3 ns. Units are color-coded as in Chart 1 except for the pyridine, which acts as a hinge and is highlighted in gold. Isobutoxy groups and solvent molecules are not shown.

dx.doi.org/10.1021/ja304322c | J. Am. Chem. Soc. 2012, 134, 11282−11288

variable lengths at positions remote from the binding site provided new insights into the parameters that determine guest binding and release rates. We showed that diastereoselectivity in these complexes occurs during the release of the guest (some complexes are more stable than others) and not during the binding (tartaric acid does not discriminate the capsule handedness from the outside). Quite remarkably, we showed that increasing the overall helix stability does not necessarily result in slower guest binding and release. On the contrary, the presence of long stable and rigid segments may result in more frequent opening of the capsule around a monomer that plays the role of a hinge. These results thus help improve the design principles of synthetic helical molecular capsules. Slowing down guest binding and release rates would require stabilization of the helix locally around the monomers that most likely act as hinges.

■ ASSOCIATED CONTENT

Supporting Information

Experimental details for synthetic procedures, spectroscopic data, crystallographic information files for **1**−**4** (CIF), and representative molecular dynamics simulations (movies). This material is available free of charge via the Internet at http://pubs.acs.org.

■ AUTHOR INFORMATION

Corresponding Author

i.huc@iecb.u-bordeaux.fr

Notes

The authors declare no competing financial interests.

■ ACKNOWLEDGMENTS

This work was supported by an ANR grant (Project No. ANR-09-BLAN-0082-01).

■ REFERENCES

(1) (a) Garric, J.; Léger, J.-M.; Huc, I. *Angew. Chem., Int. Ed.* **2005**, *44*, 1954−1958. (b) Bao, C.; Kauffmann, B.; Gan, Q.; Srinivas, K.; Jiang, H.; Huc, I. *Angew. Chem., Int. Ed.* **2008**, *47*, 4153−4156. (c) Garric, J.; Léger, J.-M.; Huc, I. *Chem.—Eur. J.* **2007**, *13*, 8454−8462. (d) Bao, C.; Gan, Q.; Kauffmann, B.; Jiang, H.; Huc, I. *Chem.—Eur. J.* **2009**, *15*, 11530−11536.

(2) Ferrand, Y.; Kendhale, A. M.; Kauffmann, B.; Grélard, A.; Marie, C.; Blot, V.; Pipelier, M.; Dubreuil, D.; Huc, I. *J. Am. Chem. Soc.* **2010**, *132*, 7858−7859.

(3) Delsuc, N.; Kawanami, T.; Lefeuvre, J.; Shundo, A.; Ihara, H.; Takafuji, M.; Huc, I. *ChemPhysChem* **2008**, *9*, 1882−1890.

(4) (a) Hou, J.-L.; Shao, X.-B.; Chen, G.-J.; Zhou, Y.-X.; Jiang, X.-K.; Li, Z.-T. *J. Am. Chem. Soc.* **2004**, *126*, 12386−12394. (b) Li, C.; Wang, G.-T.; Yi, H.-P.; Jiang, X.-K.; Li, Z.-T.; Wang, R.-X. *Org. Lett.* **2007**, *9*, 1797−1800. (c) Waki, M.; Abe, H.; Inouye, M. *Angew. Chem., Int. Ed.* **2007**, *46*, 3059−3061. (d) Abe, H.; Machiguchi, H.; Matsumoto, S.; Inouye, M. *J. Org. Chem.* **2008**, *73*, 4650−4661. (e) Xu, Y.-X.; Wang, G.-T.; Zhao, X.; Jiang, X.-K.; Li, Z.-T. *J. Org. Chem.* **2009**, *74*, 7267−7273.

(5) (a) Nishinaga, T.; Tanatani, A.; Oh, K.; Moore, J. S. *J. Am. Chem. Soc.* **2002**, *124*, 5934−5935. (b) Tanatani, A.; Hughes, T. S.; Moore, J. S. *Angew. Chem., Int. Ed.* **2002**, *41*, 325−328. (c) Petitjean, A.; Cuccia, L. A.; Schmutz, M.; Lehn, J.-M. *J. Org. Chem.* **2008**, *73*, 2481−2495. (d) Gan, Q.; Ferrand, Y.; Bao, C.; Kauffmann, B.; Grélard, A.; Jiang, H.; Huc, I. *Science* **2011**, *331*, 1172−1175. (e) Ferrand, Y.; Gan, Q.; Kauffmann, B.; Jiang, H.; Huc, I. *Angew. Chem., Int. Ed.* **2011**, *50*, 7572−7575.

(6) (a) Szabo, T.; Hilmersson, G.; Rebek, J., Jr. *J. Am. Chem. Soc.* **1998**, *120*, 6193−6194. (b) Amaya, T.; Rebek, J., Jr. *J. Am. Chem. Soc.* **2004**, *126*, 14149−14156. (c) Lledo, A.; Restorp, P.; Rebek, J., Jr. *J. Am. Chem. Soc.* **2009**, *131*, 2440−2441. (d) Ajami, D.; Rebek, J., Jr. *Nature Chem.* **2009**, *1*, 87−90.

(7) (a) Wang, B.-Y.; Rieth, S.; Badjic, J. D. *J. Am. Chem. Soc.* **2009**, *131*, 7250−7252. (b) Rieth, S.; Badjic, J. D. *Chem.—Eur. J.* **2011**, *17*, 2562−2565.

(8) Liu, S.; Gan, H.; Hermann, A. T.; Rick, S. W.; Gibb, B. C. *Nature Chem.* **2010**, *2*, 847−852.

(9) (a) Liu, X.; Chu, G.; Moss, R. A.; Sauers, R. R.; Warmuth, R. *Angew. Chem., Int. Ed.* **2005**, *44*, 1994−1997. (b) Warmuth, R.; Makowiec, S. *J. Am. Chem. Soc.* **2007**, *129*, 1233−1241.

(10) Nakazawa, J.; Sakae, Y.; Aida, M.; Naruta, Y. *J. Org. Chem.* **2007**, *72*, 9448−9455.

(11) Houk, K. N.; Nakamura, K.; Sheu, C.; Keating, A. *Science* **1996**, *273*, 627−629.

(12) Garcia, C.; Humilière, D.; Riva, N.; Collet, A.; Dutasta, J.-P. *Org. Biol. Mol.* **2003**, *1*, 2207−2216.

(13) (a) Davis, A. V.; Raymond, K. N. *J. Am. Chem. Soc.* **2005**, *127*, 7912−7919. (b) Davis, A. V.; Fiedler, D.; Seeber, G.; Zahl, A.; v. Eldik, R.; Raymond, K. N. *J. Am. Chem. Soc.* **2006**, *128*, 1324−1333.

(14) Zuccaccia, D.; Pirondini, L.; Pinalli, R.; Dalcanale, E.; Macchioni, A. *J. Am. Chem. Soc.* **2009**, *131*, 2452−2453.

(15) Umemoto, K.; Tsukui, H.; Kusukawa, T.; Biradha, K.; Fujita, M. *Angew. Chem., Int. Ed.* **2001**, *40*, 2620−2622.

(16) Rieth, S.; Hermann, K.; Wang, B.-Y.; Badjic, J. D. *Chem. Soc. Rev.* **2011**, *40*, 1609−1622.

(17) However, a fundamental difference lies in the fact that cavities in the structures of proteins and nucleic acids tend to emerge only at the level of tertiary folds, whereas in synthetic helical receptors, a simple helix, i.e., a secondary fold, may give access to a well-defined binding pocket, toward which an array of chemical functions may converge.

(18) For other tartaric acid receptors, see: (a) Garcia-Tellado, F.; Albert, J.; Hamilton, A. D. *J. Chem. Soc., Chem. Commun.* **1991**, 1761−1763. (b) Kuroda, Y.; Kato, Y.; Ito, M.; Hasegawa, J.-y.; Ogoshi, H. *J. Am. Chem. Soc.* **1994**, *116*, 10338−10339. (c) Szumna, A. *Chem.—Eur. J.* **2009**, *15*, 12381−12388. (d) Lavigne, J. J.; Anslyn, E. V. *Angew. Chem., Int. Ed.* **1999**, *38*, 3666−3669. (e) Zhao, J.; Davidson, M. G.; Mahon, M. F.; Kociok-Köhn, G.; James, T. D. *J. Am. Chem. Soc.* **2004**, *126*, 16179−16186. (f) Goswami, S.; Ghosh, K.; Mukherjee, R. *Tetrahedron* **2001**, *57*, 4987−4988.

(19) (a) Huc, I. *Eur. J. Org. Chem.* **2004**, 17−29. (b) Li, Z.-T.; Hou, J.-L.; Lib, C. *Acc. Chem. Res.* **2008**, *41*, 1343−1353. (c) Gong, B. *Acc. Chem. Res.* **2008**, *41*, 1376−1386. (d) Saraogi, I.; Hamilton, A. D. *Chem. Soc. Rev.* **2009**, *38*, 1726−1743.

(20) Jiang, H.; Léger, J.-M.; Huc, I. *J. Am. Chem. Soc.* **2003**, *125*, 3448−3449.

(21) Bakkali, H.; Marie, C.; Ly, A.; Thobie-Gautier, C.; Graton, J.; Pipelier, M.; Sengmany, S.; Léonel, E.; Nédélec, J.-Y.; Evain, M.; Dubreuil, D. *Eur. J. Org. Chem.* **2008**, 2156−2166.

(22) Kendhale, A. M.; Poniman, L.; Dong, Z.; Laxmi-Reddy, K.; Kauffmann, B.; Ferrand, Y.; Huc, I. *J. Org. Chem.* **2011**, *76*, 195−200.

(23) (a) Perrin, C. L.; Dwyer, T. J. *Chem. Rev.* **1990**, *90*, 935−967. (b) Pons, M.; Millet, O. *Prog. Nucl. Magn. Reson. Spectrosc.* **2001**, *38*, 267−324.